Analysis of stable zonal flow state bifurcations

A. Kammel, K. Hallatschek

Max-Planck-Institute for Plasma Physics, 85748 Garching, Germany

Introduction

Self-consistent resistive drift wave turbulence simulations have been utilized to examine the zonal flow transition, yielding the first finding of transport bifurcations in this system. These transport states visualized by density corrugations are linked to a zonal flow asymmetry - with steeper, more pronounced flows opposite to the electron diamagnetic drift direction.

The potential influence of drift wave turbulence can be found in the high gradient tokamak edge (at the outer rim of the H-mode internal transport barrier) as well as in geostrophic modes, constituting the drift wave analogon for planetary turbulence.

In this work, the following turbulent sheared-slab cold-ion resistive Hasegawa-Wakatani drift-wave system has been examined utilizing the two-fluid code NLET [3]:

$$d_t n = d_t \nabla_\perp^2 \phi \tag{1}$$

$$\hat{\rho}_s^{-3} d_t \nabla_\perp^2 \phi = -\partial_\parallel^2 (\phi - n) \tag{2}$$

Parameter studies

Using eqns. (1) & (2) to get the general growth rate of the shearless, non-adiabatic drift modes

$$\gamma = \Im(\omega) \propto \left[k_\perp^2 + k_\parallel^2 \left(\frac{1}{k_\perp k_y} + \frac{k_\perp}{k_y} \right)^2 \right]^{-1} \tag{3}$$

approximated by $\gamma = \omega *^2 / \omega_\parallel = k_\perp^2 / \left(k_\parallel^2 / (\hat{\rho}_s^{-3} k_\perp^2) \right) = \hat{\rho}_s^{-3} k_\perp^4 / k_\parallel^2$, a Prandtl-based mixing length estimate can be derived.

The so-found heat diffusion coefficient $D = \gamma / \vec{k}_\perp^2$ depends on the $k_\perp$ - which can be derived in the units of one of the two scales, ρ_s and $L_\perp$, e.g. in the ρ_s-dominated high-$\hat{\rho}_s$-regime:

$$D_{L_\perp}|_{k_\perp \widehat{=} \rho_s} = \frac{\gamma_{L_\perp}}{k_{L_\perp}^2}|_{k_\perp \widehat{=} \rho_s} \propto \hat{\rho}_s^{-2} \tag{4}$$

$$D_{\rho_s}|_{k_\perp \widehat{=} \rho_s} = \frac{\gamma_{\rho_s}}{k_{\rho_s}^2}|_{k_\perp \widehat{=} \rho_s} \propto \hat{\rho}_s^{0} \tag{5}$$

A similar behaviour holds true in the $L_\perp$-dominated low-$\hat{\rho}_s$-regime, with the transition between both regimes ocurring roughly at $\hat{\rho}_s \approx 0.15 - 0.20$, coinciding well with the onset of zonal flow formation. Both cases yield a simple relation between the two unit scales:

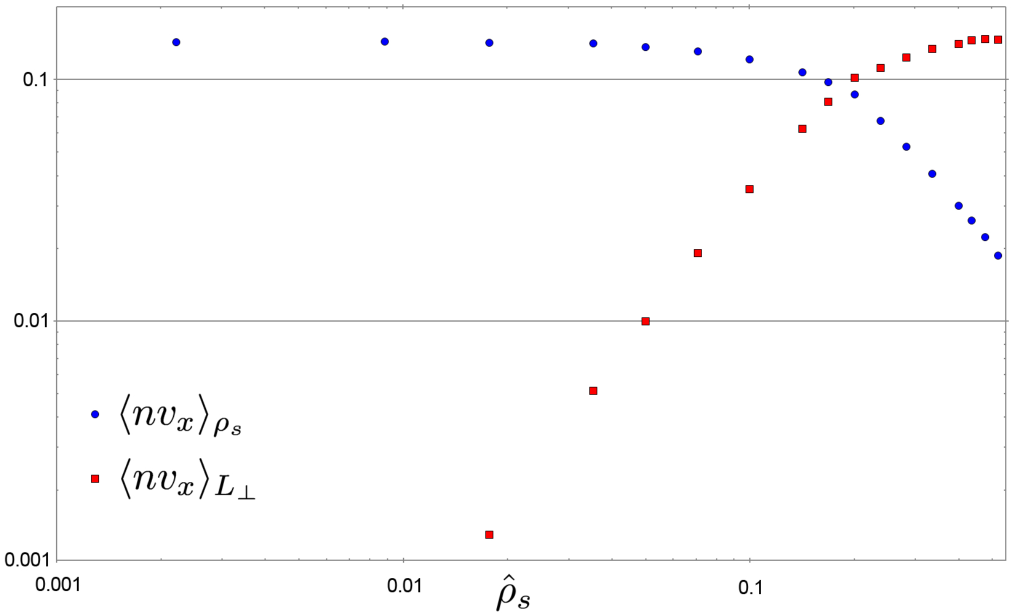

Figure 1: Density flux $\langle nv_x \rangle$ is plotted versus the dimensionless parameter $\hat{\rho}_s$ in units of the two orthogonal length scales ρ_s and $L_\perp$.

$$\frac{D_{L_\perp}}{D_{\rho_s}} = \hat{\rho}_s^{-2} \tag{6}$$

It has been verified very well by a set of computational parameter scans over $\hat{\rho}_s$ that $D_{L_\perp}$ is indeed asymptotically constant for small $\hat{\rho}_s$ and, vice versa, D_{ρ_s} for large $\hat{\rho}_s$.

Transport bifurcations

For the first time in such self-consistent drift wave turbulence simulations, transport bifurcations with two stable gradients have been discovered.

These bifurcations manifest in the form of density corrugations representing stationary transport states with regions of high gradients and low diffusivity around the sharply concentrated negative flows and broad regions of low gradients and high diffusivity in the vicinity of the broadened positive flows - the bifurcations are thus accompanied by a zonal flow asymmetry.

This flow structure typically emerges on time scales $\sim O(10^1)$ for a $\hat{\rho}_s \approx 0.28$ (gaining approximately one order of magnitude for each doubling of $\hat{\rho}_s$) - this, in addition to the necessity of an increased resolution, could explain why they have not been found in earlier studies [1].

It is important to note that the drift wave zonal flow wavelength is not pre-described (as it is for ITG based flows), with flows occurring in arbitrary scales.

Bifurcation mechanism

Using the general drift wave action invariant N [2] for the wave packet intensity

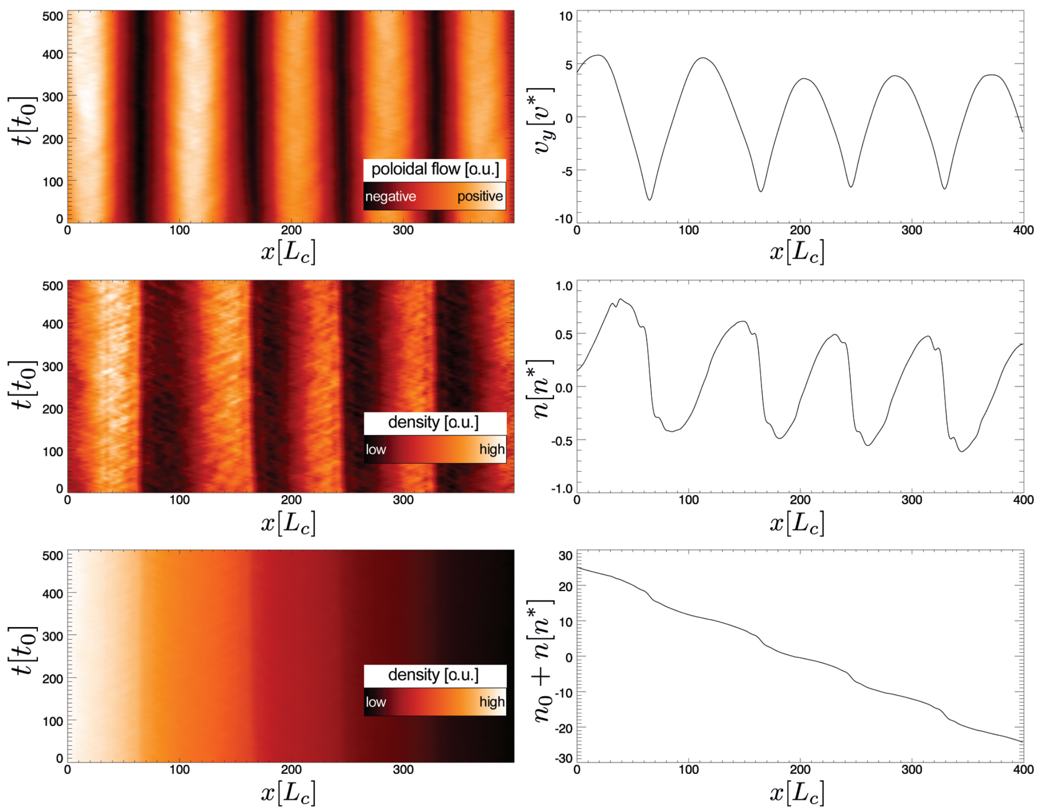

Figure 2: For $\hat{\rho}_s \approx 0.28$, poloidal flow v_y, density corrugations n and the total density gradient n_0+n are shown in a high-resolution ($n_{x,y} = 512$, $L_{x,y} = 64$) 2D plot depicting radius vs time (left hand side) next to the associated time-averages for all radii (right hand side), showcasing both the density corrugations and the flow asymmetry.

$$\partial_t N_{\vec{k}} = -\nabla_{\vec{x}} \left(N_{\vec{k}} \cdot \vec{v}_{gr,\vec{k}} \right) - \nabla_{\vec{k}} \left(N_{\vec{k}}(x) \cdot \dot{\vec{k}}(\vec{x},\vec{k}) \right) \tag{7}$$

(with the second term stemming from a shear flow which can influence the wave number locally [5] through $\dot{\vec{k}} = -\vec{\nabla}_x \vec{v} \cdot \vec{k}_0$), negative flows are seen to repulse the turbulence, while their positive counterparts exhibit attraction: The flows act like forcefields, changing the radial wavenumbers of the drift waves. Transport (aka turbulence) levels are thus reduced around the negative flows.

Since the transport balance $\partial_x \Gamma(x) = 0$ has to be maintained in equilibrium, higher gradients are required at the location of the negative flows in order to counterbalance this reduction. Density corrugations form, the steepened gradients of which leading to an increased rate of drift mode generation close to the flow minima. These drift waves are subsequently repelled by the negative flows radially, thereby exhibiting Reynolds stresses which, in turn, are able to fuel the flow. The associated carry-off of drift waves causes to a deepening of the negative flows as well as a broadening of the positive flows, yielding the described asymmetric flow pattern.

Radial streaks

For constant shear flow, turbulent drift wave eddies are observed to form radial streaks, moving down the flow gradient. The opposite would be expected, in agreement with

$$v_{gr,x,cold} = \frac{\partial \omega}{\partial k_x} = \frac{-2k_x k_y \hat{\rho}_s^2}{\left[1+\hat{\rho}_s^2(k_x^2+k_y^2)\right]^2} \quad (8)$$

where $k_x = k_{x_0} - \frac{\partial v_y}{\partial x} t|k_y|$, yielding $\frac{\partial v_{gr,x}}{\partial t} = 2v_y' k_y^2 \hat{\rho}_s^2$ (which is negative in the case of negative flow shear) and therefore uphill movement.

Four explanations are possible: Amplification via shear flow interaction (which only occurs for high wavenumbers, while generally leading to too small growth rates as $k_x \to -\infty$), acceleration in the gradient direction (which is impossible due to a ceiling $max(v_{gr,x})$ being reached soon), scattering (which occurs for high enough drift wave intensity, where the drift waves resemble shear flow optics for $k\rho_s \gtrsim 1$) and transport effects. The characteristics of the streaks' backscattering process were found to be consistent with the observed downhill movement.

However, this picture proves incomplete: For a constant density profile, the streak direction reverses, matching the initial expectations. It is only the corrugations in the density profile which cause the apparent contradiction by displacing the transport peak to such a degree that it actually stabilizes the density corrugations instead of destroying them, effectively reversing the direction in which the streaks flow - rendering the apparent contradiction a corrugation-caused transport effect.

Summary

Our sheared slab drift wave turbulence computations yield the very first example of transport bifurcations for drift wave zonal flows. These transport states as well as the associated asymmetric flow pattern constitute a robust phenomenon within an considerable parameter range, which has been explained qualitatively. Also, an apparent contradiction has been found - and resolved - in the form of downhill drift wave streaks.

References

[1] A. Zeiler, D. Biskamp, J.F. Drake and P.N. Guzdar, Phys. Plasmas **3**, 8, 2951-2960 (1996)
[2] K. Itoh, K. Hallatschek, S.-I. Itoh et al, Phys. Plasmas **12**, 062303 (2005)
[3] K. Hallatschek and A. Zeiler, Physics of Plasmas **7**, 2554 (2000)
[4] K. Hallatschek and D. Biskamp, Phys. Rev. Lett. **86**, 1223 (2001)
[5] P.H. Diamond, S.-I. Itoh, K. Itoh and T.S. Hahm, Pl. Phys. Control. Fus. **47**, 35 (2005)
[6] K. Hallatschek and A. Kammel, Submitted to Phys. Rev. Lett., (2012)